PRJ, Vol. 3 (January 1991); P. 27–34, 13 FIGS.

ACOUSTIC PROPERTIES AS FUNCTION OF DEPTH IN THE GULF OF SUEZ, EGYPT

Adel A.A. Othman* and G.H. Hamada**

خصائص انتقال الموجات الصوتية كدالة للعمق في خليج السويس بمصر

د. عادل علي علي عثمان ، د. حمادة غريب

يتعلق إضمحلال الموجات السيزمية وسرعاتها بالصفات والخصائص الطبيعية للصخور. تتغير العوامل المتحكمة في هذه الصفات معتمدة على الحالة الفيزيائية المؤثرة في الصخور.

في الدراسة الحالية ، تم إجراء مضاهاة تفصيلية بين إضمحلال وسرعة وتردد الموجات السيزمية. كذلك تم إختبار الصفات الصوتية للتغيرات الصخرية ، أما تأثير العمق على درجة الحساسية لهذه المعاملات فقد درست بالتفصيل.

ABSTRACT

Seismic wave attenuation and seismic wave velocity are related to the physical properties of rocks. The controlling factors of these properties are varying, depending upon the physical conditions of the rocks.

In the present study, a detailed correlation between the seismic wave attenuation, seismic wave velocity, and propagating frequency has been reported. The sensitivity of the acoustical parameters to the change of lithology is well tested. The effect of depth on the degree of sensitivity of these parameters is also studied.

INTRODUCTION

The relative sensitivity of velocity and attenuation as a function of lithology has been a contro-versial matter. Extensive processing and analysis of the recorded seismic data and integrating the results with geological information from other sources like well logs, can often make accurate estimates of the subsurface geology, together with lithology, depositional environment and, in some cases, the fluid content.

*Geology Dept., Al-Azhar University, Nasr City, Cairo, Egypt.
**Min. Pet. and Metal. Dept., Cairo University, Giza, Egypt.

Many attempts have been made by the seismologists throughout the history of seismic exploration, to reduce the amount of uncertainty and the number of unresolvable problems. The exact nature of the travelling seismic signal or its waveform, and its distortion and attenuation by the medium are not quite clear and are still questionable.

Vertical seismic profile (VSP) data can provide information that decrease some types of uncertainties and can help to resolve many of them. McDonal *et al.* (1958), and Tullos *et al.* (1969) have measured in-situ attenuation of seismic frequencies. Attwell *et al.* (1966) and Hamilton (1967) have conducted experiments on attenuation and they found a linear relationship between attenuation and frequency. An important contribution using VSP was made by Hauge (1981).

The objective of the present study is to measure the cumulative attenuation termed by Hauge (1981) on one VSP, the average velocity and the average frequency. These parameters were plotted against depth and were shown side by side with the composite log to emphasize the response of each parameter to variations in lithology.

GEOLOGIC SYNOPSIS

The topmost 1200 feet of the geologic section encountered in the studied well is predominantly

sandstones with a limestone bed occupying the depth interval from 1525 to 1800 feet and minor shale, limestone and anhydrite intercalations through the rest of the interval. At the base of this interval, another type of anhydrites and shales of cyclic nature starts which was deposited alternatively, with one salt intercalation. This interval goes down to a depth of 4825 feet. The depth interval from 4825 down to 7100 feet is occupied by rock salt with five minor intercalations of anhydrites and shales. Below 7100 feet and to a depth of 10 450 feet, the section is dominated by shaly sandstones with frequent thin beds of limestone sandstones with frequent thin beds of limestone through the entire depth interval. The interval includes also a 300 feet thick anhydrite-shale bed at the upper part, and another one 30 feet thick at 10 000 feet depth.

THEORETICAL CONCEPTS

The displacements associated with propagated seismic waves in a medium can be written as:

$$U_{x_2}(f)=G_x(x)U_{x_1}(f)\,e^{-\alpha x x}\,e^{i\omega(t-(x_2-x_1)/v)};\quad x_2>x_1 \qquad (1)$$

where α_x is the spatial attenuation between distance x_1 and x_2. $U_{x_1}(f)$ is the reference spectral amplitude. x is the distance difference from the reference event. v is the velocity of the propagated wave in the medium. ω is angular frequency. $G_x(x)$ is a geometrical factor which includes spherical divergence, reflections, transmissions, between distances x_1 and x_2. Knopoff (1964) and McDonal *et al.* (1958) assumed that the spatial attenuation is a linear function of frequency. In the present study, we will assume that α_x varies linearly with frequency and is expressed in decibel as:

$$\alpha_x(f)=\beta_x f/8.686 \qquad (2)$$

with:

$$\beta_x=\int_{x_1}^{x_2}\beta_0\,dx \qquad (3)$$

Where the factor β_x is a function of the separation distance (x_2-x_1), and cannot be considered as intrinsic rock property. By considering the constant Q-model in this work, this leads to express β_x as frequency independent factor.

This factor β_x will be refered as cumulative attenuation (Schoenberger *et al.*, 1978; Hauge 1981). β_0 is the interval attenuation over the separation interval $[x_1, x_2]$. It is equal to

$$\beta_0=\pi Q_i^{-1}/v_i \qquad (4)$$

where v_i is the interval velocity over the separation interval $[x_1, x_2]$ and Q_i^{-1} is the specific dissipation factor also over the same separation interval.

An important concept is the validity of the assumption that the geometric factor has the same frequency independence allower the separation interval $[x_1, x_2]$. The spatial attenuation may be expressed as function of delay time between the sample event and the reference one (Tullos *et al.*, 1969; Hauge, 1981).

By using the decibel units (dB) for calculating the interval attenuation β_0, equation (4) will take the following form:

$$\beta_0=27.2878\,Q_i^{-1}/v_i \qquad (5)$$

Combining equations (1), (2) and (3) leads to:

$$U_{x_2}(f)=G_x(x)U_{x_1}(f)\,e^{-x\beta_x f/8.686} \qquad (6)$$

The spectral ratio method is merely a rearrangement of equation (6) as:

$$\ln U_{x_2}-\ln U_{x_1}=-x\beta_x f/8.686+\ln G_x \qquad (7)$$

where U_x is now taken as the reference pulse, the pulse to which all other pulses are referenced. Equation (7) may be written as follows:

$$\ln\left(\frac{U_{x_2}}{U_{x_1}}\right)=-x\beta_x f/8.686+\ln G_x \qquad (8)$$

The ratio on the left side of equation (8) is linear with respect to frequency and has negative slope $x\beta_x$ which can be determined via least-squares technique. After values of β_x are determined for all depths, they are plotted versus depth to produce cumulative attenuation curve.

MEASUREMENT OF ACOUSTIC PROPERTIES

The lateral subsurface stratigraphic changes, related to water or petroleum presence, might be observed on surface or VSP seismic profile. In the present study a trial to measure acoustic properties at different depths in a well drilled in Gulf of Suez offshore area, to determine if significant lateral changes in stratigraphic horizons correspond to acoustic changes in these horizons.

(1) Measurement of Attenuation

Attenuation is the observed decrease in the amplitude of a transmitted seismic wave that cannot be calculated by geometric effects. Attenuation is usually a small quantity that is difficult to measure, especially

in-situ. This attenuation includes losses in amplitude due to anelastic effects and to scattering.

VSP can be used to correlate the relationship between attenuation and significant rock parameters such as sand percentage or sand–shale ratio. Therefore, attenuation can be a useful diagnostic property in seismic stratigraphy and reservoir investigations.

The relation between attenuation and lithology was made by Hauge (1981). The accuracy of the slope of cumulative attenuation curve depends on the density of observations (Spencer *et al.*, 1981).

By using Eq. (8), the estimated β_x values for all depths are plotted in Fig. 9. The cumulative attenuation, increased by increasing depths (Fig. 9). The values range from 0.025 to 0.08 dB/Hz.

(2) Predominant Frequency Calculation

Average frequency is the parameter that normally describes the predominant frequency, which is the frequency with maximum amplitude spectrum. Since higher frequencies decay faster than lower ones, this parameter is expected to decrease with travel path.

The average frequency changes with depth may be used as a measure for the wavelet shape changes also with depth. Sheriff (1983), has defined an expression for calculating the average frequency of a downhole event as follows:

$$f_{ave} = \left\{ \sum_{i=0}^{n} f_i U_x^2(f_i) \right\} \Big/ \left\{ \sum_{i=0}^{n} U_x^2(f_i) \right\} \tag{9}$$

In Eq. (9), f_{ave} is the average or predominant frequency of the wavelet at depth or distance equal to x from source. f_i is the *i*-th frequency value of the amplitude spectrum. $U_x(f_i)$ is the amplitude spectrum at distance x. The low and the upper boundaries of the summations run over all the discrete frequencies f_i up to the Nyquist frequency. The calculated average frequency are plotted against depth and shown in Fig. 10.

(3) Estimation of Average Velocity

Velocity analysis for real seismic surveys is necessary. The main sources of velocity information are the velocity log and a check-shot survey that should have been run in the borehole, and the travel time of the VSP direct wave. Kohler and Koenig (1986) found errors by comparing the calculated traveltimes of the direct wave with the traveltimes picked in the VSP records. These errors are quite clear for large offsets, while for zero offset the traveltime were correct. They explained these differences as due to a laminated structure velocity anisotropy. Salo and Schuster (1989) demonstrated that the velocity structure can be reconstructed using both reflected and direct-wave traveltimes from VSP data. The velocity errors estimated by using only direct-arrival traveltimes are 6.08% but are 4.72 percent in case of using direct- and primary-arrival traveltimes in VSP velocity inversion (when the layers are horizontal). Kennett *et al.* (1971) discussed the velocity measured from well velocity surveys and the use of calibrated acoustic logs.

In the present study, the first arrivals were detected at different levels in a well drilled in the Gulf of Suez. The average velocity along the source-receiver offset is given by the general form (Al-Chalabi, 1974):

$$v_{ave} = (1/T) \int_0^T v_{inst}(t)\, dt \tag{10}$$

where v_{inst} is the instantaneous velocity, defined as the velocity in an infinitesimally small interval, and T is the total travel time.

The next expression will be used for the average velocity along the normal incidence trajectory for the VSP data:

$$v_{ave} = (1/T_0) \sum_{n=1}^{N} v_n (t_n - t_{n-1}) \tag{11}$$

where T_0 is the total zero offset time. v_n is the *n*-th interval velocity over the interval time $[t_{n-1}, t_n]$. N is number of sample intervals. T_0 can be written as:

$$T_0 = \sum_{n=1}^{N} t_n - t_{n-1} \tag{12}$$

Figure (11) shows the average velocity measured in feet per second plotted against the depth in feet.

DATA HANDLING AND DISCUSSION

The analysed VSP, acquired off-shore in the Gulf of Suez, was digitized only for the direct, downgoing events at an equal sampling rate equal to 0.0025 second. The spectral band-width equals to 200 Hz. This sampling interval turned out to be most suitable; because spectral amplitudes at frequencies higher than 120 Hz are negligibly small. Deconvoluting the source pulse was conducted on the assumption that since the firing pressure was constant, at 120 bars, throughout the recording, the spectral ratios should eliminate its effect.

The reference pulse and the frequency range in this technique over which the cumulative attenua-

tion is calculated are chosen by trial and error. The best results were obtained, with the reference pulse at 1200 feet and a least-squares fit of the spectral amplitude ratio taken between 10 and 100 Hz. To smooth out the spectra for the effect of finite pulse duration, a time domain filter is considered. The Hanning window was used, which is given by:

$$u(t)=0.5-0.5\cos(2\pi t/T_c); \qquad 0\leqslant t\leqslant T_c \tag{13}$$

where the T_c is the truncation interval. Different time windows were tried out; e.g. the Hanning, trapezoidal, and the rectangular window. The Hanning proved to be most appropriate and did not alter the original spectral texture, at least not below 140 Hz.

The amplitude spectra were calculated using the discrete Fourier transform which is given by (Brigham, 1974)

$$U(n/Nt)=\sum_{K=0}^{N-1} u(kt)\, e^{-i2\pi nk/N} \tag{14}$$

$$n=0, 1, 2, \ldots, N-1$$

where N is the number of digits, t is the sampling interval, u(kt) is the sample amplitude, U(n/Nt) is the Fourier transform which was normalized for varying truncation intervals.

Figures 1–7 show plots of frequency spectra of the downward-travelling first arrival at different depths of 1200, 1800, 2600, 4400, 5600, 7600, and 10400 feet, respectively. The plots show the spectral amplitude in decibel which is normalized to the maximum amplitude. In general, the amplitudes have been normalized, trace by trace, so the amplitude loss due to the increase of depth cannot be seen in these figures. This can be easily seen in the composite plot in Fig. 8.

Having accepted the assumption that the attenuation is roughly proportional to frequency, the cumulative attenuation at different depths has been calculated. The overall picture of the cumulative attenuation curve increases with increasing depth. Generally, lithologic zonation can be established. Rate of cumulative attenuation increases over the intervals dominated by sandstones. On the other hand, it is relatively constant, with the rate of interval attenuation being approximately zero over the intervals occupied by anhydrites and rock salt.

Another important point is the lateral changes of the recorded event from a target stratigraphic horizon. This might indicate significant change in rock lithology like porosity build up or sand pinch out. These changes may be expressed also in frequency domain; i.e. the propagating predominant frequencies. According to Fig. 10, it is noticed that higher frequencies events are shown in shallow depths. Hence, the higher frequency events suffer small attenuation. (Figs 9 and 10).

The average velocity as a function of depth, shown in Fig. 11, could be differentiated on the basis of the curve gradient into five distinct zones, which roughly correspond to the topmost sandstone zone (from 1000 to 3200 feet), the anhydrite-shale zone (from 3200 to 4800 feet), the salt-zone (from 4800 to 7100 feet), the shaly sandstone-limestone zone (from 7100 to 9600 feet); and the bottom of sandstone zone (from 10400 to 10700 feet). No further information on the variations in lithology through each zone could be drawn from the plot.

A closer look into the fine texture of the cumulative attenuation curve, Fig. 13, reveals two outstanding phenomena that correlate well with two lithologic identities, consequently meriting some detailed discussion. First the physical unrealisable phenomenon of negative attenuation, which is confirmed by increasing average frequency. This is particularly prominent over the depth intervals 5600 to 6000 feet and 7200 to 7600 feet. On the composite log, the only common thing at these two intervals is the presence of anhydrites. This anhydrites caused some sort of compensation and attenuation to the propagated waveforms. Secondly, the leaps of cumulative attenuation values at depths equal to 1400 and 8800 feet, correspond to limestone beds. The average frequency curve, Fig. 13, shows the leap at 8800 feet which is of

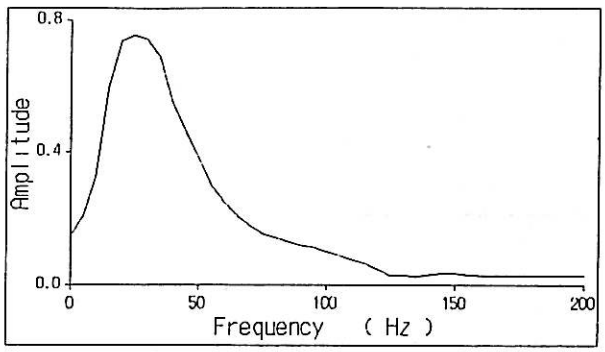


FIG. 1. Amplitude spectrum of seismic pulse at depth equal to 1200 feet.

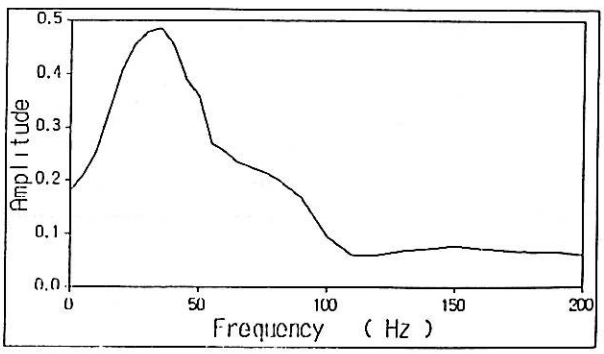


FIG. 2. Amplitude spectrum of seismic pulse at depth equal to 1800 feet.

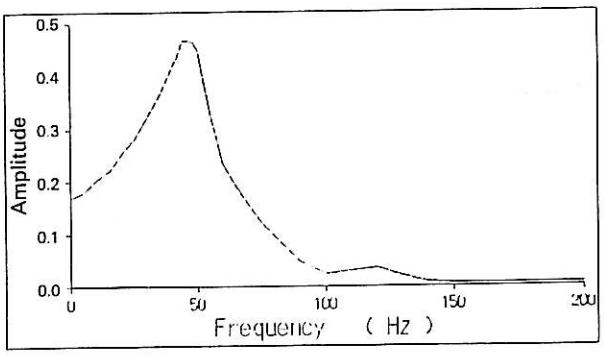


FIG. 3. Amplitude spectrum of seismic pulse at depth equal to 2600 feet.

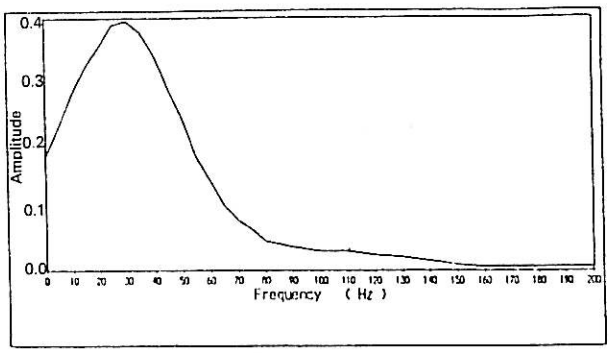


FIG. 4. Amplitude spectrum of seismic pulse at depth equal to 4400 feet.

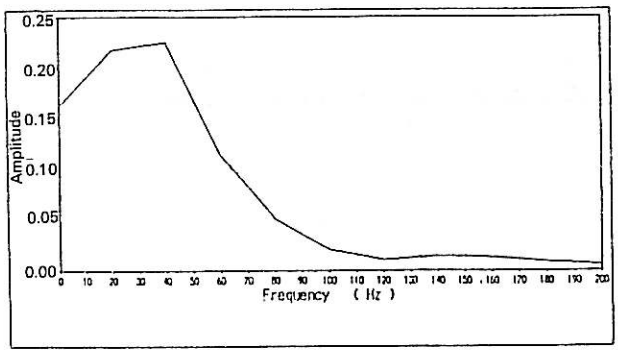


FIG. 5. Amplitude spectrum of seismic pulse at depth equal to 5600 feet.

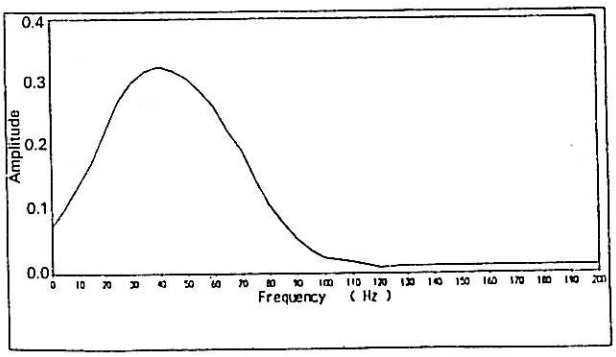


FIG. 6. Amplitude spectrum of seismic pulse at depth equal to 7600 feet.

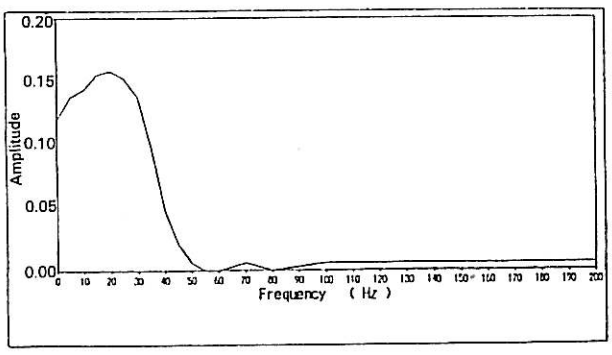


FIG. 7. Amplitude spectrum of seismic pulse at depth equal to 10400 feet.

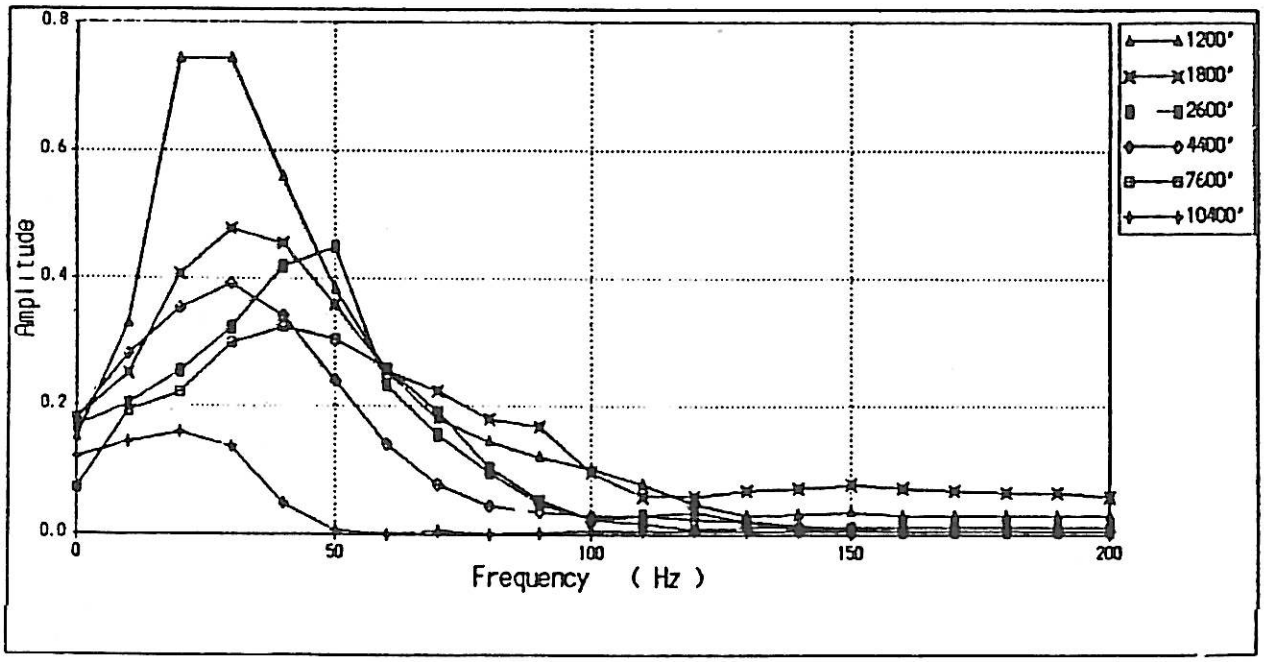


FIG. 8. Amplitude spectra of seismic pulses at some selected depths equal to 1200, 1800, 2600, 4400, 7600, and 10400 feet.

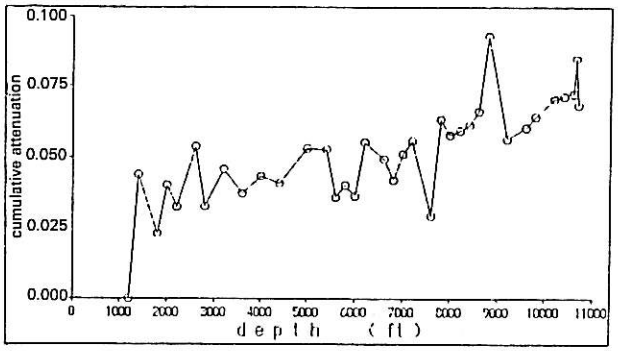


FIG. 9. Cumulative attenuation at different depths calculated over the frequency interval 10–100 Hz.

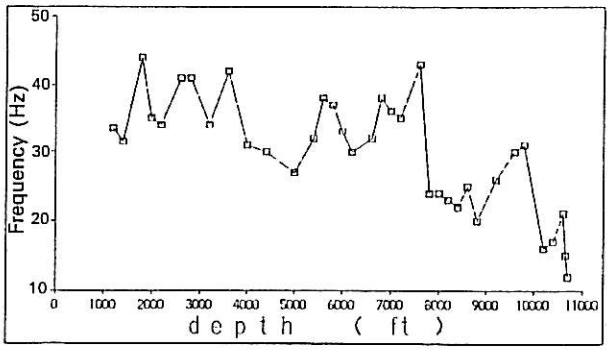


FIG. 10. Predominant frequency calculated over the frequency interval 10–100 Hz.

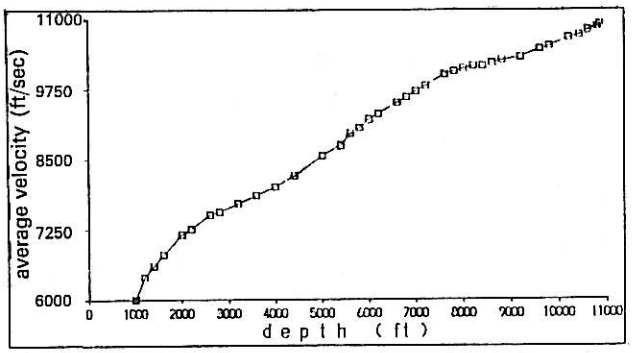


FIG. 11. Average velocity calculated as function of depth in a Well drilled in Gulf of Suez.

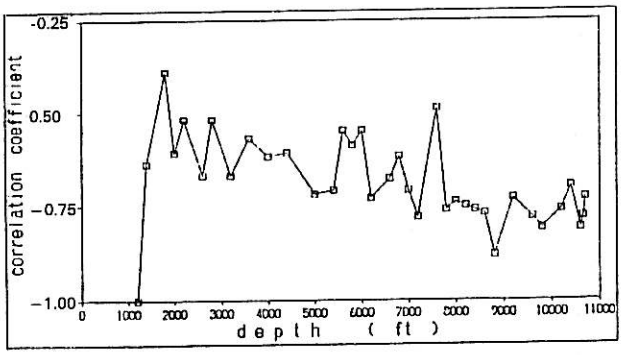


FIG. 12. Correlation coefficients calculated over the frequency interval 10–100 Hz, at selected depths.

a magnitude less than that at 1400 feet, as normally expected for attenuation which tends to decrease with depth due to increasing confining pressure.

The correlation coefficient of the determined attenuation is plotted faced to the geologic composite log (Fig. 12). Their values range between 0.5 up to 0.75, and have increased as cumulative attenuation and depth increased.

CONCLUSION

Attenuation represented by the cumulative attenuation is a far mere sensitive parameter to variation in lithology than velocity and frequency. Two lithologic identities were associated with two prominent phenomena on the cumulative curve. Anhydrites were associated with the phenomenon of negative attenuation and were interpreted as responsible for partial compensation of attenuated downhole pulses.

Limestones were engaged to sudden jumps in values of cumulative attenuation with lower average frequencies, and were interpreted as sources of high attenuative effects. An evident point scatter is shown on the average frequency.

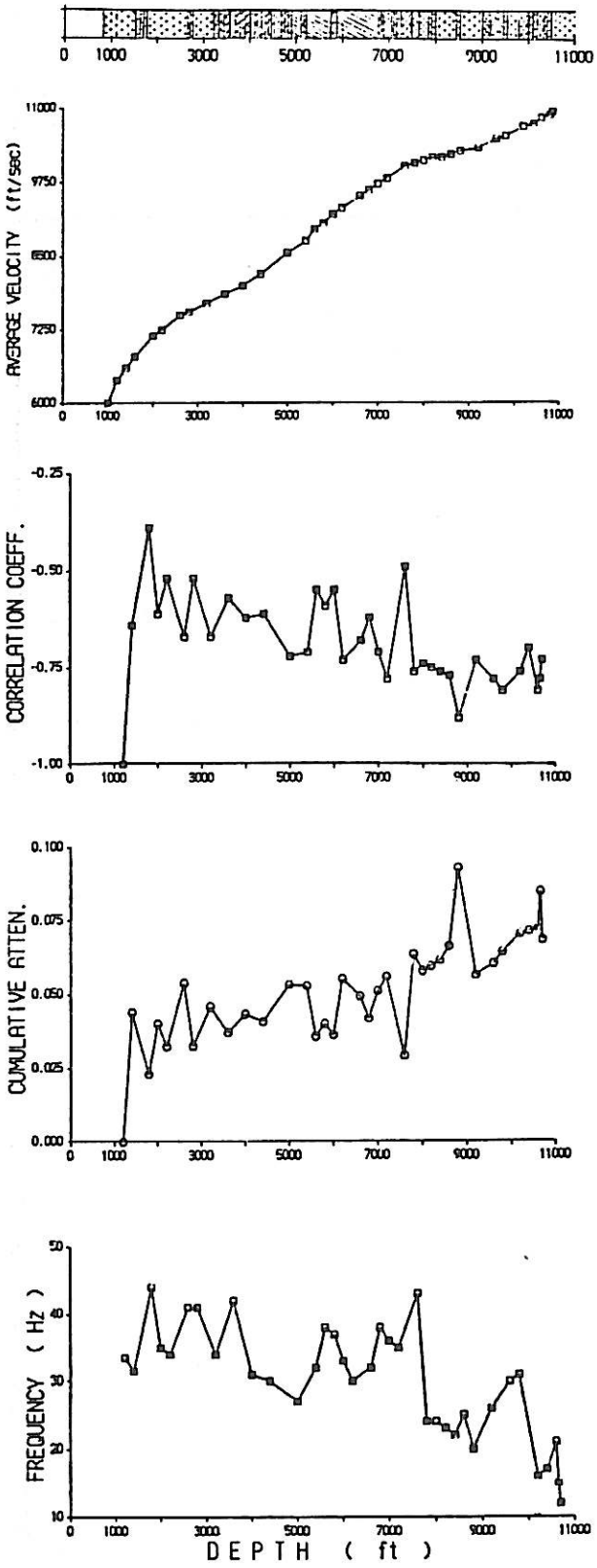


FIG. 13. The average frequency, cumulative attenuation, average velocity, and correlation coefficients as function of depth, correlated with the geologic log.

REFERENCES

Al-Chalabi M., 1974, An analysis of stacking, rms, average, and interval velocities over a horizontal layered ground. *Geoph. Prosp.*, v. 22, p. 458–475.

Attwell P.B. and Ramana Y.V., 1966, Wave attenuation and interval friction as function of frequency in rocks. Geophysics, v. 31, p. 1049–1056.

Brigham E.O., 1974, The fast Fourier transform, Prentice-Hall, Inc., 252 page.

Hamilton E.L., 1976, Sound attenuation as a function of depth in the sea floor. *Acoust. Soc. Am. J.*, v. 59, p. 528–535.

Hauge P.S., 1981, Measurements of attenuation from vertical seismic profiles. *Geophysics*, v. 46, p. 1548–1558.

Kennett P. and Ireson R.L., 1971, Recent developments in well velocity surveys and the use of calibrated acoustic logs. *Geophys. Prosp.*, v. 19, p. 395–411.

Knopoff L., 1964, *Q. Rev. Geophys. Res.*, 2, p. 625–660.

Kohler K. and Koenig K., 1986, Reconstruction of reflecting structures from vertical seismic profiles with a moving source. *Geophysics*, v. 51, p. 1923–1938.

McDonal F.J., Angona F.A., Mills R.L., Sengbush R.L., van Nostrand R.G. and White J.E., 1958, Attenuation of shear and compressional waves in Pierre shale. *Geophysics*, v. 23, p. 412–439.

Salo E.L. and Schuster G.T., 1989, Traveltime inversion of both direct and reflected arrivals in vertical seismic profile data. *Geophysics*, v. 54, p. 49–56.

Sheriff R.E., 1983, Encyclopedic dictionary of exploration geophysics. 2nd edition, SEG, Tulsa.

Spencer T.C., Sonnad J.R. and Butler T.M., 1982, Seismic Q-Stratigraphy or dissipation. *Geophysics*, v. 47, p. 16–24.

Tullos F.N. and Reld A.C., 1969, Seismic attenuation of Gulf Coast sediments. *Geophysics*, v. 34, p. 516–528.